Polymer Chemistry

PAPER

View Article Online
View Journal | View Issue

Cite this: *Polym. Chem.*, 2018, **9**, 4994

Peptide–dendron hybrids that adopt sequence-encoded β-sheet conformations†

Deborah A. Barkley,[a] Sang Uk Han,[a] Tadanori Koga [a,b] and Jonathan G. Rudick *[a]

Received 13th June 2018,
Accepted 10th September 2018

DOI: 10.1039/c8py00882e

rsc.li/polymers

Rational design rules for programming hierarchical organization and function through mutations of monomers in sequence-defined polymers can accelerate the development of novel polymeric and supramolecular materials. Our strategy for designing peptide–dendron hybrids that adopt predictable secondary and quaternary structures in bulk is based on patterning the sites at which dendrons are conjugated to short peptides. To validate this approach, we have designed and characterized a series of β-sheet-forming peptide–dendron hybrids. Spectroscopic studies of the hybrids in films reveal that the peptide portion of the hybrids adopts the intended secondary structure.

Introduction

Peptides and proteins are tremendous resources for introducing tunable functionality in synthetic polymeric materials. Conjugating polymers to peptides and proteins compensates for the imperfect control over monomer sequence and chain length afforded by modern polymerization methods.[1–3] The precise sequence of amino acid residues of the peptide/protein domain confers hybrid polymers with emergent functions such as molecular recognition, catalysis, and therapeutic activity.[4–9] Synthetic and genetic methods make interrogation of these complex functions possible through site-specific mutations to the amino acid sequence.[10–12] The predictable folding and self-assembly of peptides is especially valuable in programming the hierarchical assembly of hybrid polymers.[13–19]

Greater control over molecular structure can be gained by combining peptides with dendrons[20,21] or other sequence-defined polymers. The diverse pool of α-amino acid monomers can enrich the programmable functionality of dendrons by conferring chirality,[22–24] molecular recognition,[25] surface adsorption,[26] and stimulus responsive properties[27–33] to peptide–dendron hybrids. The homogeneity of hybrids obtained from monodisperse polymers may be advantageous for applications as therapeutics.[21,34] Peptide-mediated intermolecular hydrogen-bonding provides mechanisms for supramolecular polymerization of peptide–dendron hybrids into anisotropic nanostructures.[35–41] In particular, several macrocyclic peptide–dendron hybrids[42,43] and dendritic dipeptides[44–49] have been shown to self-organize into periodically ordered arrays of porous columnar structures in bulk. The design principles gained from studies of dendritic dipeptides have been successfully applied to the design of other, non-peptidic self-assembled nanostructures.[50,51] The porous cylindrical nanostructures obtained from self-assembling dendritic dipeptides are functional mimics of channel proteins.[44,52,53]

Inspired by the tunability and processability afforded by combinations of peptides with dendrons, we have investigated hybrids of dendrons with an α-helical bundle-forming peptide.[32,33,54,55] The defined arrangement of different amino acids in the core of an α-helix bundle motif could allow us to synthesize chemical gradients or unique binding sites within supramolecular dendrimers. We recently reported examples of α-helix bundle-forming peptide–dendron hybrids that self-organize in an hexagonally ordered array of columns.[54] We found that the helix bundle stoichiometry in the liquid crystalline mesophase matches the stoichiometry of the bundle formed by the peptide in aqueous buffer. This remarkable correspondence implies that folding and self-assembly instructions encoded by the amino acid sequence persist in the non-biological environment of the liquid crystalline mesophase.

To further validate that design rules from biochemical studies of peptides and proteins can be applied to bulk self-organized materials, we have characterized a series of β-sheet peptide–dendron hybrids **1–4** (Fig. 1). The same dendrons from our self-organizable α-helix bundle-forming peptide–dendron hybrids have been conjugated to a seven-residue, β-sheet-forming peptide. Infrared (IR) and circular dichroism (CD) spectra of hybrids **1–4** confirm that the peptide adopts

[a]*Department of Chemistry, Stony Brook University, Stony Brook, New York 11794, USA. E-mail: jon.rudick@stonybrook.edu*
[b]*Department of Materials Science and Engineering, Stony Brook University, Stony Brook, New York 11794, USA*

†Electronic supplementary information (ESI) available. See DOI: 10.1039/c8py00882e

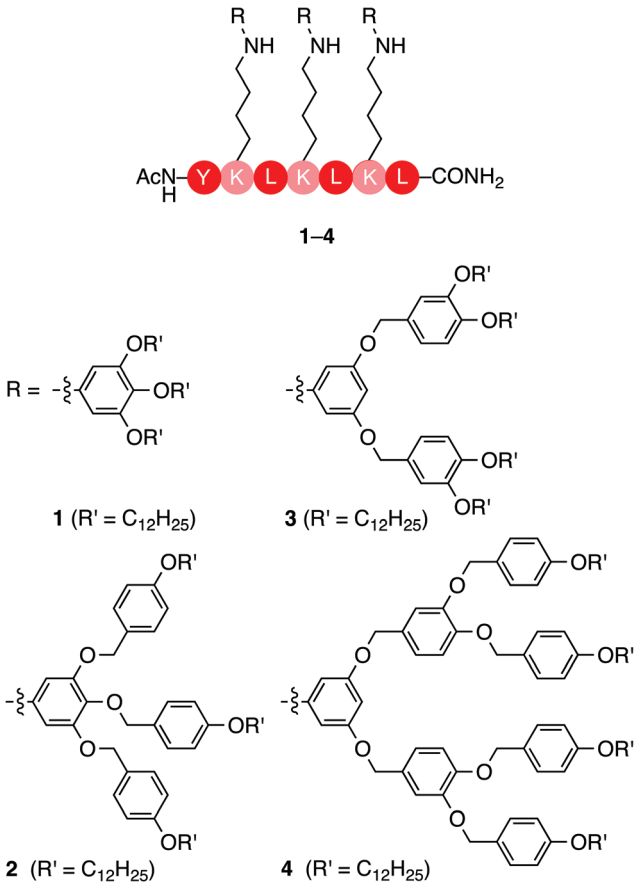

Fig. 1 Structures of the β-sheet peptide–dendron hybrids **1–4**. Amino acids are designated by single-letter codes: Y = tyrosine, K = lysine, and L = leucine.

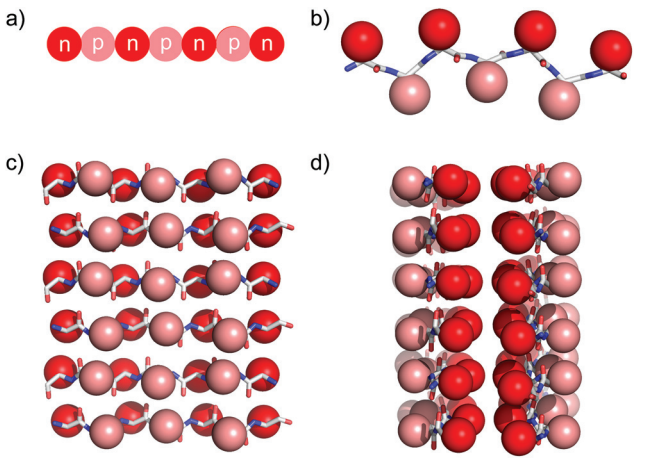

Fig. 2 (a) Pattern of non-polar (n, red color) and polar (p, pink color) amino acids employed in the design of β-sheet-forming peptides. (b) Schematic model of a peptide in the extended β-strand conformation with colored spheres indicating the relative orientation of the side chains. (c) Schematic model of an antiparallel β-sheet assembly of the peptide designed by hydrophobic patterning. (d) Packing of the non-polar faces of two β-sheet assemblies.

the β-sheet conformation encoded in the amino acid sequence. These results support our expectation that transport and binding properties programmed by the primary sequence of amino acids in proteins can be integrated in peptide–dendron hybrid materials.

Results and discussion

Design rationale

The sequence of amino acids in peptide–dendron hybrids **1–4** was designed based on a rudimentary implementation of hydrophobic patterning. An alternating arrangement of non-polar (n) and polar (p) amino acids encodes the β-sheet secondary structure (Fig. 2a).[56] In an extended conformation, the non-polar residues make up one face of the β-strand and the polar residues make up the other face (Fig. 2b). Intermolecular hydrogen-bonding between the backbone amide groups assembles the β-strands into a β-sheet that amplifies the amphiphilic character of the β-strands (Fig. 2c). Sequestration of the non-polar faces of the β-sheets provides an additional driving force for β-sheets to assemble in a face-to-face manner (Fig. 2d). Polar residues on the exterior of such a putative β-sheet assembly serve as the points of attachment for the dendrons.

Lysine (K) and leucine (L) were chosen as the polar and non-polar amino acids, respectively. The same polar and non-polar residues were used in our previously reported α-helical bundle-forming peptide–dendron hybrids.[32,33,54,55] The side-chain amino group of each lysine residue is efficiently acylated using dendritic pentafluorophenyl esters.[54] DeGrado and Lear have shown that a seven-residue peptide with alternating leucine and lysine residues self-assembles into a β-sheet structure in buffered aqueous solution.[56] The N-terminus of the peptide was acetylated to ensure that the dendrons would be conjugated exclusively through the side-chains of the lysine residues. The C-terminus of the peptide was amidated. Tyrosine (Y) was used as the N-terminal non-polar residue to provide a convenient spectroscopic probe from which we could identify the peptide in HPLC experiments and determine the amount of peptide in aqueous solutions.[57] Thus we arrived at AcNH-YKLKLKL-$CONH_2$ (**5**) as the β-sheet-forming peptide to which we planned to conjugate the self-assembling dendrons.

Peptide–dendron hybrids **1–4** have dendrons grafted to the side-chain of each lysine residue *via* an amide functional group. Conjugating self-assembling dendrons to the polar residues of a β-sheet-forming peptide disrupts the amphiphilic character of the β-sheet-forming peptide. Nonetheless, the extended β-strand conformation should be one of the lowest energy conformations of the peptide–dendron hybrids.[58] We envision that, in the solid and melt states, macromolecular crowding effects replace the hydrophobic drive forces that underlie self-assembly of β-sheet-forming peptides in aqueous solution. When the peptide portion adopts an extended β-strand conformation, the hybrids have an overall anisotropic

shape that should pack more efficiently than other conformations with a less ordered arrangement of the dendrons.

Synthesis of the peptide–dendron hybrids

Peptide–dendron hybrids **1–4** were prepared by grafting the dendrons to the peptide. An advantage of this approach is that the peptide and dendrons can be purified to homogeneity using methods that are standard for the respective materials, which helps to minimize undesired products that need to be separated from the desired peptide–dendron hybrids. Acylation of the side-chain amino group in each lysine residue of **5** was accomplished using dendritic pentafluorophenyl esters (Scheme 1). The efficient amidation reaction between amines and pentafluorophenyl esters makes pentafluorophenyl esters excellent reagents for ligation of polymers with proteins[59,60] and dendrons with peptides.[26,54]

The acylation reactions were performed in a mixture of DMF and THF (1 : 1 v/v) at 50 °C to fully solubilize the reactants, intermediates, and products. Pentafluorophenyl esters **6–9** are only moderately soluble in DMF (*i.e.*, a good solvent for **5**) and very soluble in THF (*i.e.*, a poor solvent for **5**). Because the pentafluorophenyl ester was used in excess ($[dendron]_0/[amine]_0 = 1.5/1$; $[\mathbf{5}]_0 = 0.01$ M), we judged the reactions to be complete when we could no longer observe **5** or partially dendronized intermediates in MALDI-TOF mass spectra of aliquots taken from the reaction mixture. Peptide–dendron hybrids **1–4** were isolated in good yields (75–96%) using flash column chromatography.

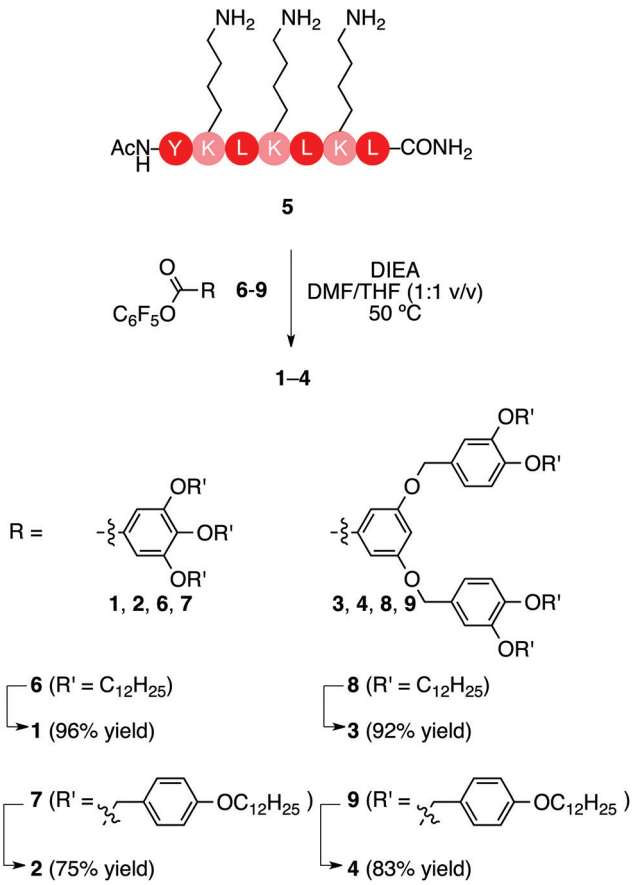

Scheme 1 Graft-to synthesis of peptide–dendron hybrids **1–4**.

Table 1 Molecular weight characteristics of the hybrids **1–4**

Hybrid	m/z[a]	M_n[b]	M_w/M_n[b]
1	2938.3646[c] 2954.3011[d]	3020	1.05
2	3892.9287[c] 3908.9287[d]	4160	1.07
3	4127.3669[c] 4143.3208[d]	4120	1.08
4	5401.1574[c]	6130	1.09

[a] Determined from MALDI-TOF mass spectra. [b] Determined from GPC in THF (1 mL min^{-1}, 40 °C) calibrated with polystyrene standards. [c] $[M + Na]^+$ ion. [d] $[M + K]^+$ ion.

The identity of the peptide–dendron hybrids was confirmed primarily from MALDI-TOF mass spectra. We observed very good agreement (±0.5 Da) between the exact and observed masses for the Na^+ and K^+ adducts in MALDI-TOF mass spectra of hybrids **1–3** (Table 1). The resolution of these spectra was sufficient to show agreement between the simulated and observed isotope distributions for the $[M + Na]^+$ ions (Fig. 3a–c). The MALDI-TOF mass spectrum of **4** was of overall lower quality (Fig. 3d) than the spectra of the other hybrids, which accounts for the poorer agreement (±2 Da) between the calculated and found masses. The chemical shift values in ^{1}H NMR spectra of hybrids **1–4** varied between sample preparations, which is probably due to aggregation of the hybrids in solution. Nonetheless, there was generally good agreement between integration values for the resonance assigned to the protons of N-terminal acetyl group (δ 2.5–2.0 ppm), and the broad resonance assigned to the methyl groups of the leucine side-chain and aliphatic tails of the dendrons (δ 0.88 ppm). The spectroscopic data are consistent with the structures of hybrids **1–4** shown in Fig. 1.

The purity of the peptide–dendron hybrids was confirmed primarily from the elution profile in GPC experiments. Fig. 4 shows that peptide–dendron hybrids **1–4** each elute as a single species. The number-average molecular weight (M_n) values calculated from the GPC elution profiles increase according to the size of the conjugated dendrons (Table 1). Peptide–dendron hybrids **2** and **3** are close enough in molecular weight that they are essentially indistinguishable in the GPC experiments. The narrow molecular weight distribution (M_w/M_n) values calculated from the chromatograms (Table 1) are consistent with hybrids **1–4** each being isolated as monodisperse, sequence-defined macromolecules. We observe no mass peaks at m/z-values below the mass peaks from the ionized hybrids in lower resolution MALDI-TOF mass spectra of hybrids **1–4** (Fig. S1†). The GPC and MALDI data support that **1–4** are defect-free macromolecules.

IR spectra of the hybrids

Assignments of the infrared (IR) bands that are unique to the backbone amide groups of the peptide–dendron hybrids

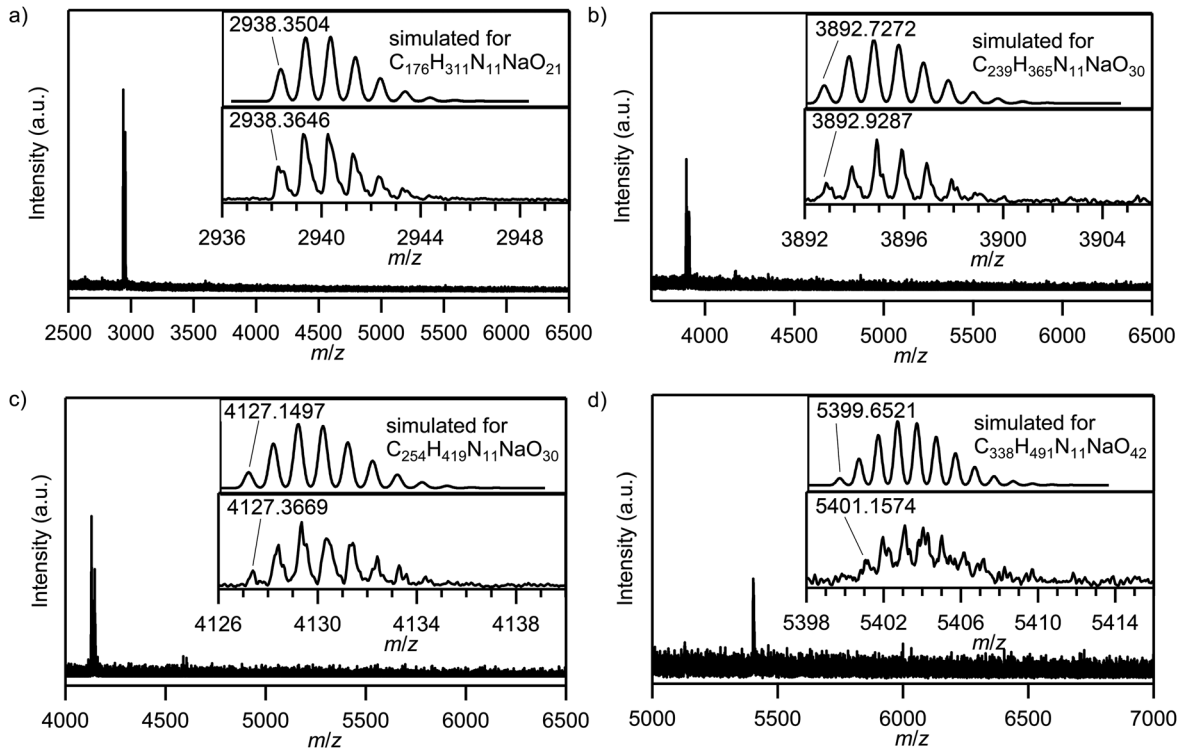

Fig. 3 MALDI-TOF mass spectra of peptide–dendron hybrids (a) **1**, (b) **2**, (c) **3**, and (d) **4**. The inset compares the simulated isotope pattern[61] (upper) with the observed isotope distribution (lower) for the $[M + Na]^+$ ion.

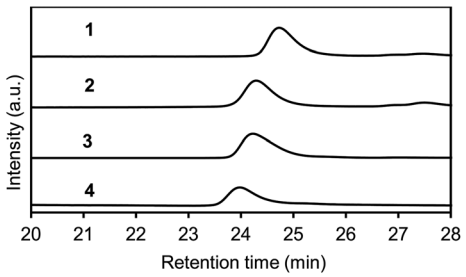

Fig. 4 Elution profiles of hybrids **1–4** from GPC in THF (1 mL min^{-1}, 40 °C).

can provide significant insight with regard to the conformation of the peptide portion of the molecules. The C═O stretching (amide I) and the N–H in-plane bending (amide II) modes are sensitive to the environment of the amide group. The amide I band, in particular, is distinctly different for peptides in an α-helical conformation (1660–1648 cm^{-1}) and in a β-sheet conformation (1640–1628 cm^{-1}).[62] Contributions from the side-chain amides and aromatic rings to the IR spectra of hybrids **1–4** are expected in the region of the amide I band from the main-chain of the peptide.

IR spectra of hybrids **1–4** were acquired in the solid state. Films of the hybrids were spin-cast from CH_2Cl_2 onto a salt plate. The IR spectra of hybrids **1–4** in the region between 1750–1500 cm^{-1} is shown in Fig. 5, and the absorptions assigned to the amide I and amide II bands are reported in Table 2. The amide I absorption in hybrids **1–4** appears at 1628–1627 cm^{-1}, which is substantially different than the amide I bands we observed in α-helical peptide–dendron hybrids (*i.e.*, 1655–1651 cm^{-1}).[54] The position of the amide I band for each hybrid matches what is expected for a peptide in the β-sheet conformation. In the IR spectra of peptide–dendron hybrid **4** (Fig. 5) and of peptide **5** (Fig. S4†) we were able to identify a second, much weaker amide I absorption at 1673 cm^{-1}, which is sometimes observed in antiparallel β-sheet assemblies. The IR spectra are consistent with the peptide–dendron hybrids adopting the designed secondary structure in the solid state.

To determine whether the observed amide I and amide II absorptions are unique to the main-chain amides, we characterized the dendritic butyl amides **10–13** (Fig. 6). Compounds **10–13** are models for the dendronized lysine side-chain in the peptide–dendron hybrids. The IR spectra from spin-cast films **10–13** were better resolved than the spectra of **1–4**. The N–H stretching band of the amide (a.k.a., amide A band) was clearly identified in the spectra of **10–13** (Table 3), and was used to confirm that the benzamides are hydrogen bonded in the solid state. By comparing the spectra of **10–13** with the IR spectra of dendritic ester inter-

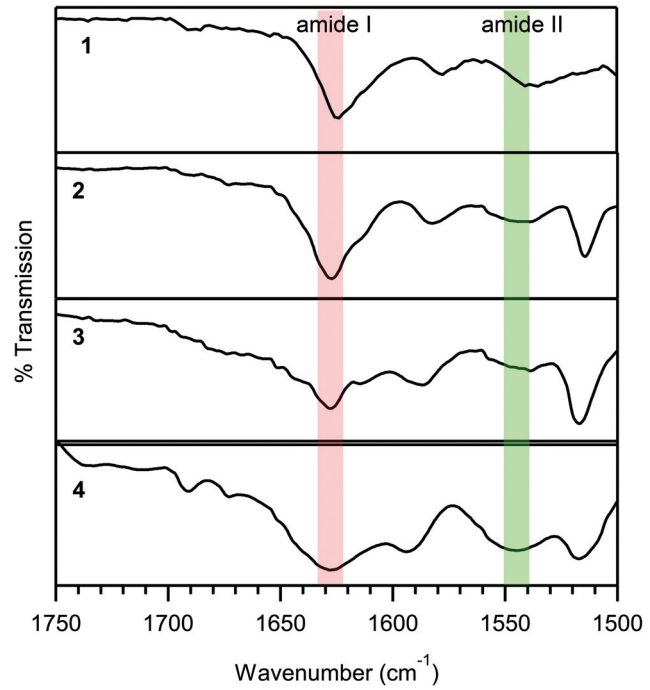

Fig. 5 Infrared spectra of peptide–dendron hybrids **1–4** acquired at room temperature from spin-cast films.

Table 2 Amide I and Amide II bands of peptide–dendron hybrids **1–4**

Hybrid	Amide I (cm^{-1})	Amide II (cm^{-1})
1	1628	1546
2	1628	1540
3	1627	1540
4	1628, 1673	1543

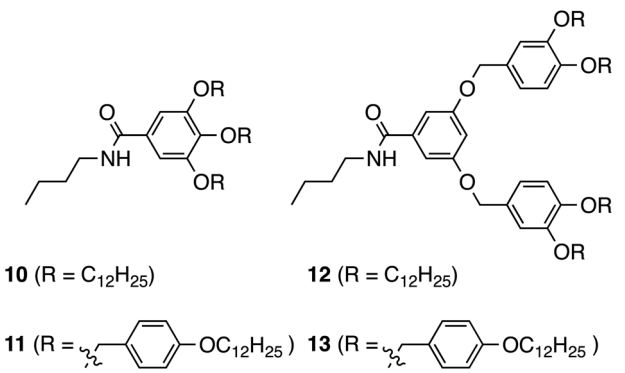

Fig. 6 Structures of the dendritic butyl amides **10–13**.

mediates from the syntheses of **6–9** (Fig. S9†), we were able to identify those absorptions arising from the C=C stretching modes of the aromatic rings as well as the amide I and amide II bands of the amide. We have reported in Table 3 the bands we assigned to each of these vibrational modes.

Table 3 Assignments of the C=C and amide vibrational modes of the dendritic monobenzamides **10–13**

Monobenzamide	Amide A (cm^{-1})	Amide I (cm^{-1})	C=C (cm^{-1})	Amide II (cm^{-1})
10	3236	1629	1580, 1503	1555
11	3290	1638	1613, 1582, 1513	1544
12	3249	1638	1590, 1519	1547
13	3268	1633	1613, 1589, 1516	1548

The amide I and amide II bands of **10–13** occur at higher energy and are more variable than those of the peptide–dendron hybrids **1–4**. We infer from the IR spectra of **10–13** that the side-chain amide contributes to the amide I and amide II bands in the spectra of **1–4**.

CD spectra of the hybrids

β-Sheet and α-helix conformations of peptides can be readily distinguished in CD spectra.[63] The β-sheet conformation is characterized by a maximum at 195 nm from the amide π–π* transition and a minimum at 218 nm from the amide n–π* transition.[64] There is good agreement between spectra acquired in solution and film states.[54,56] The self-assembling dendrons in **1–4** introduce two potential problems for the straightforward interpretation of peptide secondary structure from CD spectra of the hybrids. First, contributions from aromatic groups in the side-chains of peptides can alter the sign and shape of the observed CD spectrum.[65] Second, linear dichroism arising from anisotropic order of the hybrids contributes to the observed CD spectrum from solid films.[66] We found that, for α-helix bundle-forming peptide–dendron hybrids,[54] the self-assembling dendrons made only minor contributions to the CD spectra of the hybrids.

The CD spectra obtained from films of hybrids **1–4** (Fig. 7) are similar to the CD spectra of β-sheet peptides. The spectra show minima in the range 215–230 nm. A maximum below 200 nm is also visible in the spectrum of hybrid **1** (Fig. 7a). There is no maximum in the far-UV region of the CD spectra of hybrids **2–4**, which could be due contributions from the aromatic chromophores in the dendrons. We previously noted that some chirality transfer from the α-helical peptide to the dendrons was evident in the far-UV CD spectra of α-helix bundle-forming peptide–dendron hybrids.[54] The magnitude of the CD spectra (per residue) are weaker for β-sheet peptides than for α-helical peptides, which may also account for a greater contribution from the dendrons to the CD spectra of hybrids **1–4**. Importantly, the CD spectra in Fig. 7 are significantly different from the CD spectra of α-helix bundle-forming peptide–dendron hybrids bearing the same dendrons.[54] The CD spectra are consistent with hybrids **1–4** forming β-sheet structures in the solid state, and agree well with the CD spectrum obtained from a film of **5** (Fig. S4†).

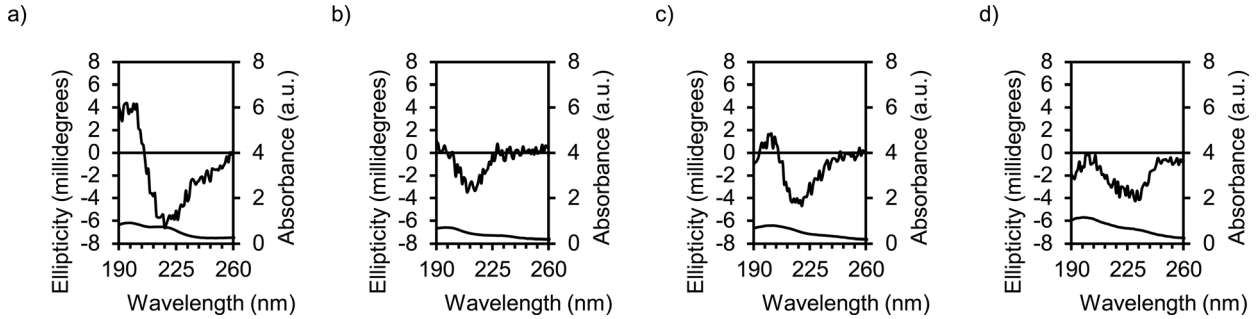

Fig. 7 Circular dichroism spectra (upper curve, left-hand axis) and UV-vis spectra (lower curve, right-hand axis) from films of (a) **1**, (b) **2**, (c) **3**, and (d) **4** on quartz. Spectra were recorded at 20 °C.

Conclusion

Rudimentary protein design rules offer a foundation from which to construct functional materials *via* programmable hierarchical organization of peptide–dendron hybrids. The recent report of self-organizable α-helix bundle-forming peptide–dendron hybrids[32,33,54,55] is a promising starting point because natural helix bundles exhibit diverse functionality.[67,68] Indeed, functional hybrid materials based on α-helix bundle-forming peptide-polymer conjugates have validated the concept of designing binding sites for light-harvesting chromophores in polymeric films.[69] To confirm that the amino acid sequence helps determine the secondary structure of the peptide–dendron hybrids, we have investigated rationally designed β-sheet-forming peptide–dendron hybrids. The spectroscopic studies reported herein strongly support the successful rational design of β-sheet structures in the peptide–dendron hybrids. In conjunction with our previous spectroscopic studies of related α-helical peptide–dendron hybrids,[54] these results provide compelling evidence that protein design rules are applicable to bulk phases of peptide–dendron hybrid materials.

Conflicts of interest

There are no conflicts of interest to declare.

Acknowledgements

Acknowledgement is made to the National Science Foundation (DMR-1255245 (J. G. R.), and CMMI-1332499 (T. K.) for support of this research. We also thank Prof. Daniel P. Raleigh (Stony Brook University) for providing access to a circular dichroism spectrometer. The MALDI-TOF mass spectra in Fig. 3 were acquired by Dr. Robert Rieger (Stony Brook University Proteomics Center) on a mass spectrometer that was funded by a shared instrumentation grant (NIH/NCRR 1 S10 RR023680-1).

References

1 J.-F. Lutz, J.-M. Lehn, E. W. Meijer and K. Matyjaszewski, *Nat. Rev. Mater.*, 2016, **1**, 16024.
2 I. Cobo, M. Li, B. S. Sumerlin and S. Perrier, *Nat. Mater.*, 2014, **14**, 143–159.
3 B. Jung and P. Theato, *Adv. Polym. Sci.*, 2012, **253**, 37–70.
4 A. S. Carlini, L. Adamiak and N. C. Gianneschi, *Macromolecules*, 2016, **49**, 4379–4394.
5 A. C. Obermeyer and B. D. Olsen, *ACS Macro Lett.*, 2015, **4**, 101–110.
6 D. Y. W. Ng, Y. Wu, S. L. Kuan and T. Weil, *Acc. Chem. Res.*, 2014, **47**, 3471–3480.
7 J. Y. Shu, B. Panganiban and T. Xu, *Annu. Rev. Phys. Chem.*, 2013, **64**, 631–657.
8 S. Lecommandoux and É. Garanger, *C. R. Chim.*, 2016, **19**, 143–147.
9 Y. J. Yang, A. L. Holmberg and B. D. Olsen, *Annu. Rev. Chem. Biomol. Eng.*, 2017, **8**, 549–575.
10 L. Raibaut, O. El Mahdi and O. Melnyk, *Top. Curr. Chem.*, 2015, **363**, 103–154.
11 M. Paradi-Bas, J. Tulla-Puche and F. Albericio, *Chem. Soc. Rev.*, 2016, **45**, 631–654.
12 J. A. Johnson, Y. Y. Lu, J. A. Van Deventer and D. A. Tirrell, *Curr. Opin. Chem. Biol.*, 2010, **14**, 774–780.
13 R. Hourani, C. Zhang, R. van der Weegen, L. Ruiz, C. Li, S. Keten, B. A. Helms and T. Xu, *J. Am. Chem. Soc.*, 2011, **133**, 15296–15299.
14 M. L. Koh, K. A. Jolliffe and S. Perrier, *Biomacromolecules*, 2014, **2014**, 11.
15 M. J. Glassman and B. D. Olsen, *Macromolecules*, 2015, **48**, 1832–1842.
16 D. Chang and B. D. Olsen, *Polym. Chem.*, 2016, **7**, 2410–2418.
17 C. N. Lam, H. Yao and B. D. Olsen, *Biomacromolecules*, 2016, **17**, 2820–2828.
18 S. R. Diegelmann, N. Hartman, N. Markovic and J. D. Tovar, *J. Am. Chem. Soc.*, 2012, **134**, 2028–2031.
19 H.-A. Klok, G. W. M. Vandermeulen, H. Nuhn, A. Rösler, I. W. Hamley, V. Castelletto, H. Xu and S. S. Sheiko, *Faraday Discuss.*, 2005, **128**, 29–41.

20 M. A. Zhuravel, N. E. Davis, S. T. Nguyen and I. Koltover, *J. Am. Chem. Soc.*, 2004, **126**, 9882–9883.
21 G. G. Kochendoerfer, S.-Y. Chen, F. Mao, S. Cressman, S. Traviglia, H. Shao, C. L. Hunter, D. W. Low, E. N. Cagle, M. Carnevali, V. Gueriguian, P. J. Keogh, H. Porter, S. M. Stratton, M. C. Wiedeke, J. Wilken, J. Tang, J. J. Levy, L. P. Miranda, M. M. Crnogorac, S. Kalbag, P. Botti, J. Schindler-Horvat, L. Savatski, J. W. Adamson, A. Kung, S. B. H. Kent and J. A. Bradburne, *Science*, 2003, **299**, 884–887.
22 H. Shao, J. W. Lockman and J. R. Parquette, *J. Am. Chem. Soc.*, 2007, **129**, 1884–1885.
23 V. Percec, M. Peterca, A. E. Dulcey, M. R. Imam, S. D. Hudson, S. Nummelin, P. Adelman and P. A. Heiney, *J. Am. Chem. Soc.*, 2008, **130**, 13079–13094.
24 B. M. Rosen, C. Roche and V. Percec, *Top. Curr. Chem.*, 2013, **333**, 213–253.
25 X. Chen, Y. He and M. Lee, *J. Am. Chem. Soc.*, 2016, **138**, 5773–5776.
26 T. Gillich, E. M. Benetti, E. Rakhmatullina, R. Konradi, W. Li, A. Zhang, A. D. Schlüter and M. Textor, *J. Am. Chem. Soc.*, 2011, **133**, 10940–10950.
27 H. Frisch, J. P. Unsleber, D. Lüdeker, M. Peterlechner, G. Brunklaus, M. Waller and P. Besenius, *Angew. Chem., Int. Ed.*, 2013, **52**, 10097–10101.
28 H. Shao, N. A. Bewick and J. R. Parquette, *Org. Biomol. Chem.*, 2012, **10**, 2377–2379.
29 H. Shao and J. R. Parquette, *Angew. Chem., Int. Ed.*, 2009, **48**, 2525–2528.
30 D. Spitzer, L. L. Rodrigues, D. Straßburger, M. Mezger and P. Besenius, *Angew. Chem., Int. Ed.*, 2017, **56**, 15461–15465.
31 T. S. Kale, J. E. Marine and J. D. Tovar, *Macromolecules*, 2017, **50**, 5315–5322.
32 J. E. Marine, S. Song, X. Liang, M. D. Watson and J. G. Rudick, *Chem. Commun.*, 2015, **51**, 14314–14317.
33 J. E. Marine, S. Song, X. Liang and J. G. Rudick, *Biomacromolecules*, 2016, **17**, 336–344.
34 T. Wang, Y. Wu, S. L. Kuan, O. Dumele, M. Lamla, D. Y. W. Ng, M. Artz, J. Thomas, J. O. Mueller, C. Barner-Kowollik and T. Weil, *Chem. – Eur. J.*, 2015, **21**, 228–238.
35 W.-D. Jang and T. Aida, *Macromolecules*, 2003, **36**, 8461–8469.
36 K. Sato, Y. Itoh and T. Aida, *Chem. Sci.*, 2014, **5**, 136–140.
37 K.-S. Moon, E. Lee, Y.-b. Lim and M. Lee, *Chem. Commun.*, 2008, **43**, 4001–4003.
38 J. Lee, J. M. Kim, M. Yun, C. Park, J. Park, K. H. Lee and C. Kim, *Soft Matter*, 2011, **7**, 9021–9026.
39 M. von Gröning, I. de Feijter, M. C. A. Stuart, I. K. Voets and P. Besenius, *J. Mater. Chem. B*, 2013, **1**, 2008–2012.
40 P. Ahlers, H. Frisch, D. Spitzer, Z. Vobecka, F. Vilela and P. Besenius, *Chem. – Asian J.*, 2014, **9**, 2052–2057.
41 R. Appel, J. Fuchs, S. M. Tyrrell, P. A. Korevaar, M. C. A. Stuart, I. K. Voets, M. Schönhoff and P. Besenius, *Chem. – Eur. J.*, 2015, **21**, 19257–19264.
42 K. Sato, Y. Itoh and T. Aida, *J. Am. Chem. Soc.*, 2011, **133**, 13767–13769.
43 M. Amorín, A. Pérez, J. Barberá, H. L. Ozores, J. L. Serrano, J. R. Granja and T. Sierra, *Chem. Commun.*, 2014, **50**, 688–690.
44 V. Percec, A. E. Dulcey, V. S. K. Balagurusamy, Y. Miura, J. Smidrkal, M. Peterca, S. Nummelin, U. Edlund, S. D. Hudson, P. A. Heiney, H. Duan, S. N. Magonov and S. A. Vinogradov, *Nature*, 2004, **430**, 764–768.
45 V. Percec, A. Dulcey, M. Peterca, M. Ilies, Y. Miura, U. Edlund and P. A. Heiney, *Aust. J. Chem.*, 2005, **58**, 472–482.
46 V. Percec, A. E. Dulcey, M. Peterca, M. Ilies, J. Ladislaw, B. M. Rosen, U. Edlund and P. A. Heiney, *Angew. Chem., Int. Ed.*, 2005, **44**, 6516–6521.
47 B. M. Rosen, M. Peterca, K. Morimitsu, A. E. Dulcey, P. Leowanawat, A.-M. Resmerita, M. R. Imam and V. Percec, *J. Am. Chem. Soc.*, 2011, **133**, 5135–5151.
48 V. Percec, A. E. Dulcey, M. Peterca, M. Ilies, S. Nummelin, M. J. Sienkowska and P. A. Heiney, *Proc. Natl. Acad. Sci. U. S. A.*, 2006, **103**, 2518–2523.
49 V. Percec, A. E. Dulcey, M. Peterca, M. Ilies, M. J. Sienkowska and P. A. Heiney, *J. Am. Chem. Soc.*, 2005, **127**, 17902–17909.
50 V. Percec, M. R. Imam, M. Peterca, D. A. Wilson and P. A. Heiney, *J. Am. Chem. Soc.*, 2009, **131**, 1294–1304.
51 V. Percec, M. R. Imam, M. Peterca, D. A. Wilson, R. Graf, H. W. Spiess, V. S. K. Balagurusamy and P. A. Heiney, *J. Am. Chem. Soc.*, 2009, **131**, 7662–7677.
52 M. S. Kaucher, M. Peterca, A. E. Dulcey, A. J. Kim, S. A. Vinogradov, D. A. Hammer, P. A. Heiney and V. Percec, *J. Am. Chem. Soc.*, 2007, **129**, 11698–11699.
53 A. J. Kim, M. S. Kaucher, K. P. Davis, M. Peterca, M. R. Imam, N. A. Christian, D. H. Levine, F. S. Bates, V. Percec and D. A. Hammer, *Adv. Funct. Mater.*, 2009, **19**, 2930–2936.
54 D. A. Barkley, Y. Rokhlenko, J. E. Marine, R. David, D. Sahoo, M. D. Watson, T. Koga, C. O. Osuji and J. G. Rudick, *J. Am. Chem. Soc.*, 2017, **139**, 15977–15983.
55 J. E. Marine, X. Liang, S. Song and J. G. Rudick, *Biopolymers*, 2015, **104**, 419–426.
56 W. F. DeGrado and J. D. Lear, *J. Am. Chem. Soc.*, 1985, **107**, 7684–7689.
57 C. N. Pace, F. Vajdos, L. Fee, G. Grimsley and T. Gray, *Protein Sci.*, 1995, **4**, 2411–2423.
58 G. N. Ramachandran, C. Ramakrishnan and V. Sasisekharan, *J. Mol. Biol.*, 1963, **7**, 95–99.
59 S. McRae, X. Chen, K. Kratz, D. Samanta, E. Henchey, S. Schneider and T. Emrick, *Biomacromolecules*, 2012, **13**, 2099–2109.
60 K. T. Wiss, O. D. Krishan, P. J. Roth, K. L. Kiick and P. Theato, *Macromolecules*, 2009, **42**, 3860–3863.
61 M. Strohalm, mMass 5.5.0, http://www.mmass.org/ (accessed June 1, 2015).
62 M. Jackson and H. M. Mantsch, *Crit. Rev. Biochem. Mol. Biol.*, 1995, **30**, 95–120.

63 N. J. Greenfield, *Nat. Protoc.*, 2006, **1**, 2876–2890.
64 E. S. Pysh, *Proc. Natl. Acad. Sci. U. S. A.*, 1966, **56**, 825–832.
65 R. W. Woody, *Biopolymers*, 1978, **17**, 1451–1467.
66 Y. Wu, H. W. Huang and G. A. Olah, *Biophys. J.*, 1990, **57**, 797–806.
67 B. Apostolovic, M. Danial and H.-A. Klok, *Chem. Soc. Rev.*, 2010, **39**, 3541–3575.
68 D. N. Woolfson, *Adv. Protein Chem.*, 2005, **70**, 79–112.
69 A. D. Presley, J. J. Chang and T. Xu, *Soft Matter*, 2011, **7**, 172–179.